Journal of Thermal Analysis and Calorimetry, Vol. 75 (2004) 857–865

THERMAL ANALYSIS AND EPR STUDIES OF CARBON BLACK OXIDATION IN THE PRESENCE OF COPPER LOADED Y_2O_3–CeO_2–ZrO_2 CATALYST

J. F. Lamonier[1]*, *S. P. Kulyova*[2], *V. V. Lunin*[2], *E. A. Zhilinskaya*[1] *and* *A. Aboukaïs*[1]

[1]Laboratoire de Catalyse et Environnement, EA 2598, Université du Littoral-Côte d'Opale, MREID, 145, Avenue Schumann, 59140 Dunkerque Cedex, France
[2]Laboratory of Catalysis and Gas Electrochemistry, Chemistry Department, Lomonosov Moscow State University, Leninskie Gory, 119899 Moscow, Russia

(Received June 16, 2003; in revised form July 7, 2003)

Abstract

The activity of copper-free and copper-loaded $10Y_2O_3$–$10CeO_2$–$80ZrO_2$ solid solutions towards carbon black combustion was studied using simultaneous thermogravimetric analysis and differential thermal analysis techniques coupled with gas chromatography. It was demonstrated that all studied catalysts lower the temperature of carbon black combustion. The selectivity of the catalytic reaction in CO_2 formation was 100%. The comparison of electron paramagnetic resonance (EPR) spectra of pure catalysts with those of the samples (catalysts mixed with carbon black) after catalysis allowed to evidence, despite of the strong oxidizing atmosphere, a thermal reduction by carbon of Fe^{3+} (impurities), Cu^{2+} and Zr^{4+} during the reaction. Moreover a new EPR signal appeared after catalytic test and was attributed to the presence of paramagnetic metal–carbon or/and metal–sulphur complexes.

Keywords: carbon black, catalytic oxidation, ceria, copper, DTA/TG, EPR, yttrium, zirconia

Introduction

Internal-combustion engines (both gasoline- and diesel-fueled) are known to significantly contribute to air pollution. Ecological benefits of diesel engines, such as low greenhouse gas emissions, are balanced by high emission of NO_x and solid particles, mainly soot.

Soot emission can be controlled by placing a porous ceramic filter downstream for collection of solid particles. Soot, deposited on the filter, must be periodically burnt down to avoid an increase of back pressure in exhaust gas. However, such a regeneration of the filter requires high temperatures (higher than those of the exhaust

---

* Author for correspondence: E-mail: lamonier@univ-littoral.fr

1388–6150/2004/ $ 20.00
© 2004 Akadémiai Kiadó, Budapest

Akadémiai Kiadó, Budapest
Kluwer Academic Publishers, Dordrecht

gases and, hence, the filter). A low soot ignition temperature can be achieved using oxidation catalysts such as single metal oxides and mixed oxide systems [1–3] or eutectic mixtures based on oxides [4, 5]. Oxidation catalysts can be either added to the fuel in the form of soluble compounds or coated onto the internal surface of the filter [6]. In the former case, the catalyst is incorporated into the soot particles during their formation. In the latter case, the accumulated soot is oxidized in the filter.

In recent years, special attention has been focused on application of ceria (CeO_2), structurally doped with zirconia (ZrO_2), for the treatment of emissions from car engines. In comparison with pure CeO_2, the thermal stability, redox properties and catalytic activity of these solids are strongly enhanced. These special properties are explained by the substitution of Ce^{4+} by Zr^{4+} into the CeO_2 lattice, which favors the creation of structural defects and results in the acceleration of oxygen diffusion. This higher mobility of lattice oxygen is related to the phase modification of CeO_2–ZrO_2 oxides from tetragonal into cubic form. Moreover, the incorporation of yttrium (as Y^{3+}) in the CeO_2–ZrO_2 lattice promotes the stabilization of a single homogeneous cubic phase (especially in $10YO_{1.5}$–$10CeO_2$–$80ZrO_2$ [7]). The presence of anionic vacancies on the Y_2O_3–CeO_2–ZrO_2 ternary oxide surface provides special interaction with the impregnated active phase, which could induce particular catalytic activity [8].

The purpose of this work is to study, by thermal analysis, catalytic properties of $10YO_{1.5}$–$10CeO_2$–$80ZrO_2$ ternary oxide doped with copper in the combustion of carbon black to evidence a role of the oxide support (which is in pure cubic phase and, therefore, it is expected to be efficient oxygen exchanger in the reaction). The electron paramagnetic resonance has been used to characterize the different samples before and after the catalytic test.

Experimental

Preparation of samples

The support of the following composition (in mol%) $10YO_{1.5}$–$10CeO_2$–$80ZrO_2$ (denoted as Y-10) was prepared by co-precipitation technique. It was synthesized by means of adding NH_4OH solution to a solution containing the mixture of $Y(NO_3)_3{\cdot}6H_2O$, $Ce(NO_3)_3{\cdot}6H_2O$ and $ZrO(NO_3)_2{\cdot}6H_2O$ salts with desired Y:Ce:Zr ratio and total concentration of ions equals to 0.2 mol L^{-1} (pH was about 10.5–11). The prepared gel was washed with deionized water and then with a solution of ethanol (40%), dried at 373–393 K (5 h) and calcined at 823 K in a muffle furnace (5 h). The characterization of Y-10 support has already been developed in a previous paper [7]. XRD analysis revealed the formation of a single cubic phase indexed in the Fm3m space group. The cell parameter was calculated as 5.167 Å and the crystallite size evaluated at 10 nm.

The catalysts with 0.5, 1 or 3 mass% of copper were prepared by impregnation of the support with a solution of $Cu(NO_3)_2{\cdot}6H_2O$ followed by drying and calcination in air at 523 K.

Catalytic tests

The combustion of Carbon Black (CB), N330 supplied by Degussa, model of soot [6] (BET surface area is 80 m^2 g^{-1}; content of hydrocarbons, C_{12}–C_{22} alkanes, is 1 mass%), was studied with simultaneous thermogravimetric analysis (TG) and differential thermal analysis (DTA) using Netzsch STA 409 apparatus. Indeed TG and DTA methods allow a quick evaluation of catalytic activity of different solids in carbon particles oxidation [9, 10]. We used 0.05 g of the mixtures of catalyst with CB (80 and 20 mass%, respectively), which were obtained by mechanical mixing in a ball miller for 40 min. Before mixing, all the catalysts were activated at 873 K.

The reaction mixture was loaded in an alumina crucible and heated from ambient temperature to 873 K (5 K min^{-1}) in air flow (75 mL min^{-1}). The analysis of combustion products was performed with use of Varian 3600 chromatograph coupled with the thermobalance [3]. Two chromatography columns (one inside the other: CTRI Alltech) were used for separation of components of gas mixture (air, O_2, N_2, CO and CO_2). The outer column was filled with molecular sieve while the inner one with adsorbent Porapak. Operating conditions were as follows: temperature of columns was 348 K, temperature of thermoconductivity detector was 423 K (~180 mA), carrier-gas was helium (20 mL min^{-1}).

Electron paramagnetic resonance (EPR)

EPR spectra were recorded at 293 and 77 K with a Bruker EMX spectrometer operating in the X band microwave frequency (~9.5–9.7 GHz). The magnetic field was modulated at 100 kHz. The *g*-factor values were determined by simultaneous measuring the microwave frequency with high precision and the magnetic field. All EPR spectra were treated with Bruker WINEPR program, and Bruker SimFonia program was used for simulating of EPR spectra.

Results and discussion

Catalytic oxidation of carbon black

The activity of the catalysts was considered due to their ability to decrease the combustion temperature of CB in air, which in the absence of catalysts occurs in the ~800–900 K range [3]. The temperature of the first DTA peak was chosen as a characteristic of catalytic activity of the samples. The data of thermal experiments are listed in Table 1. Note that in all cases, selectivity of the reaction in CO_2 formation was 100%.

All the DTA curves consisted of two exothermic peaks. The first one was narrow and sharp, whereas the second appearing at higher temperatures, was broad and smooth (for example, DTA curve for 3%Cu/Y-10 in Fig. 1a). The most important mass loss on the TG curves was observed in the temperature range corresponding to the first DTA peak (a fast process), whereas a smaller mass loss was found for temperature area of the second DTA peak (a slow process).

Table 1 Values of temperature of first DTA maximum (T_{max}) and mass loss obtained from DTA-TG experiments in air flow for CB+catalyst mixtures

Sample	Surface area, m^2/g	T_{max}/K	Mass loss for 1st and 2nd DTA peaks/%		
			1st peak	2nd peak	Both peaks
CB+Y-10	70	749	12.2	7.2	19.4
CB+0.5%Cu/Y-10	55	712	15.5	7.4	22.9
CB+1%Cu/Y-10	43	703	15.6	6.4	22.0
CB+3%Cu/Y-10	38	694	16.0	4.7	20.7

Figure 1 compares the DTA curve (Fig. 1a) with DTG curve (time derivative of TG curve) (Fig. 1b) for 3%Cu/Y-10 sample. A very good mutual accordance between both curves indicates that each of the two DTA peaks is a chemical reaction, which is not accompanied by other chemical reactions or physical transformations. Indeed, in case of several chemical reactions either in the absence or presence of physical transformations, the corresponding DTA peak is the result of thermal effects of all these processes, and therefore DTA and DTG curves must show different changes. It is obvious that the presence of both DTA peaks is related to the oxidation of CB. The evidence is the formation of the combustion product (CO_2) in the temperature ranges of both first and second DTA peaks as well as the appearance of the curve corresponding to the rate of the CO_2 formation (Fig. 1c), coinciding according to its shape and temperature position with appropriate DTA curve (Fig. 1a).

In the absence of other chemical processes (e.g. partial oxidation of carbon), the quantity of generated heat owing to $C+O_2=CO_2$ exothermic reaction is proportional to

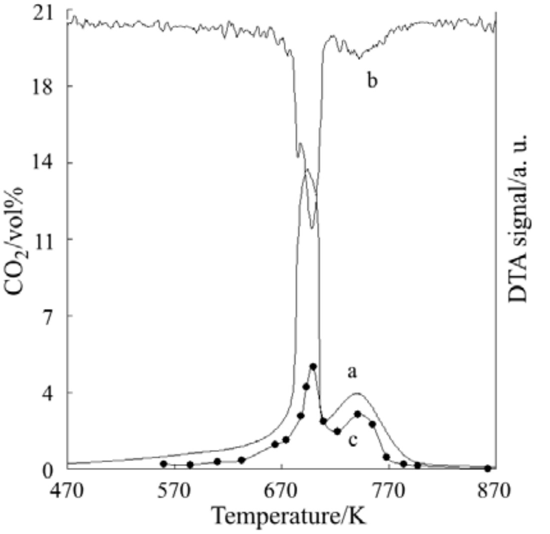

Fig. 1 DTA curve (a) and DTG curve (b) for the mixture of CB with 3%Cu/Y-10 catalyst in air flow and CO_2 current concentration (c) measured during the DTA test

the amount of CO_2 formed as a result of this reaction. Obviously, the quantity of heat generated at each of two stages of the reaction must be comparable with the CO_2 amount formed at these stages. The integration of corresponding peaks has shown that the first/second peak area ratio was higher for DTA peak as compared with that for the CO_2 peak (e.g., Figs 1a and 1c). The observable disproportion between peak areas on the two double-peak curves can be a consequence of overheating the samples at the beginning of their oxidation. Indeed, the first stage of CB oxidation reaction is very fast. Apparently, heat production and heat accumulation during this stage are more pronounced than during the second slower oxidation stage, and this can lead to overheating the sample and, hence, to the additional emission of heat [11]. Pruvost *et al*. [3] have shown that the first rapid oxidation phenomenon concerns carbon particulate in tight contact with the catalyst whereas the second one (slow oxidation) implies carbon particulate for which the contact is rather loose with the catalyst despite the 40 min mixing time.

Moreover the total mass loss during the reaction was more than 20% in the presence of copper (Table 1). Considering that transition metal oxides are often involved in a redox mechanism during catalytic CB oxidation [3, 12], the phenomenon can be attributed to the thermal reduction by carbon of metal ions.

It is worth noticing that activity of Cu-containing catalysts correlated with content of supported copper and the most active catalyst (3%Cu/Y-10) exhibited the lowest surface area (Table 1). The highest activity and the lowest surface area are well explained by the formation of CuO particles on the catalyst surface. Apparently, a promising inhibition effect, related to the decrease of surface area (from 55 to 38 $m^2\ g^{-1}$), is balanced by the high catalytic potential of CuO in CB oxidation. Indeed, in the same reaction, Pruvost *et al*. [3] clarified the role of small CuO particles, whose presence on oxide supports (besides isolated copper species) appeared as a determining parameter *vs.* the activity.

Analysis of EPR spectra of catalysts before and after catalysis

EPR spectra of initial catalysts (not mixed with carbon black) were recorded after preliminary calcination (at 873 K) in air with the subsequent outgassing ($\sim 3\cdot 10^{-5}$ mbar). Figure 2 shows the spectra recorded at 77 K.

The spectrum of Y-10 support consists of three signals denoted as A, B and C. A signal at g=4.29 with peak-to-peak width ΔH_{pp}=24.4 G is attributed to high spin Fe^{3+} ions ($3d^5$ electronic configuration, $^6S_{5/2}$ ground state, S=5/2) with low symmetry crystalline field of ligands [13]. B signal is an axial anisotropic spectrum with poorly resolved hyperfine structure. The EPR parameters ($g_\perp$=2.068, $g_\parallel$=2.277, $A_\parallel$=150 G) are characteristic of isolated Cu^{2+} ions ($3d^9$) in distorted octahedral coordination [7]. Fe^{3+} and Cu^{2+} species are present in the support as impurities. C signal represents an axial symmetry spectrum with the following parameters: $g_\perp$=1.973, $g_\parallel$=1.953. It can be attributed to Zr^{3+} ions ($4d^1$) in an octahedral environment with strong tetragonal distortion [13–15]. The Zr^{3+} ions can be formed during synthesis of the support, probably, due to dehydration of a hydroxide mixture (OH^- groups can play the role of a reducing agent for Zr^{4+} species in hydrated sample [13, 15]).

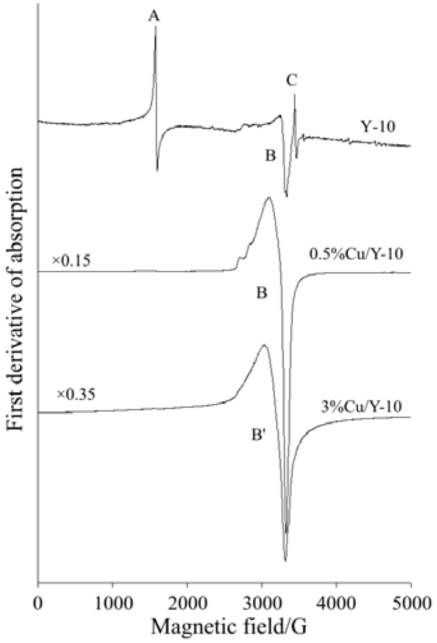

Fig. 2 EPR spectra of initial catalysts (not mixed with carbon black) calcined at 873 K, recorded at 77 K. (Intensities of spectra normalized for sample mass)

In the spectrum of 0.5%Cu/Y-10 catalyst, the B signal (with EPR parameters $g_{\|}$=2.24, $A_{\|}$=153 G, $g_{\perp}$=2.05, $A_{\perp}$=15 G and g_{iso}=2.112) is dominant. The contribution of A and C signals is negligible. Attribution of B signal to octahedral Cu^{2+} complexes is in agreement with the data of diffuse reflectance electronic spectrum investigation [7]. The value of integrated intensity of B signal corresponds to all copper present in the solid [7].

As to 3%Cu/Y-10 catalyst, the enhancement of the deposited metal content was accompanied by decreasing the Cu^{2+} ions signal intensity and by the broadening of the hyperfine structure due to a dipole–dipole interaction. A new anisotropic signal B' ($g_{\perp}$=2.1; $A_{\perp}$~12 G; $g_{\|}$=2.3; $A_{\|}$~115 G) is observed. The parameters of this signal are similar to those of Cu^{2+} ions remaining in the solid after soft CO reduction [7]. The decrease of the signal intensity with copper concentration can be explained by the formation of CuO aggregates on the solid surface from Cu^{2+} ions which leads to disappearance of isolated Cu^{2+} on the surface responsible for B signal. Indeed, when the concentration of copper(II) increases on the solid surface, the distance between the species decreases and leads to the formation of CuO particles. These latter species are undetectable by EPR due to antiferromagnetic character of the CuO solid.

EPR spectra (Fig. 3) of the catalysts mixed with carbon black after their use in the catalytic oxidation (final temperature reaction was 873 K) were recorded at 77 K after preliminary outgassing (~$4\cdot10^{-5}$ mbar). The spectrum of Y-10 support is composed of 4 signals: A, B and C signals described above and attributed to the Fe^{3+}, Cu^{2+} and Zr^{3+} ions, respectively, and a new very intense broad structureless X signal (parameters are

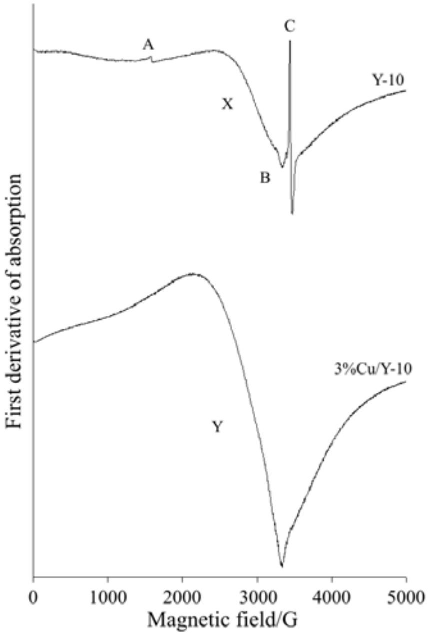

Fig. 3 EPR spectra of the samples (catalyst+CB) after catalytic test, recorded at 77 K. (Intensities of spectra normalized for sample mass)

given in Table 2). X signal can be related to the presence of paramagnetic form of residual carbon or/and sulphur compounds or/and metal–carbon or/and metal–sulphur complexes [16]. In the case of 3%Cu/Y-10 sample, A and C signals are not visible near a new Y signal because of their low relative intensity due to the presence of copper species. The Y signal is a superposition of X signal and another one more probably attributed to copper–carbon or/and copper–sulfur complexes. Table 2 shows the values of *g*-factors, the peak-to-peak line widths (ΔH_{pp}), and relative integral intensities of X and Y signal (evaluated as $I(\Delta H_{pp})^2$, where I represents the line amplitude) for the used catalysts. The nature of X and Y paramagnetic centers remains uncertain. Similar signals have been observed in EPR spectra of Cu–Ce–Al–O catalysts used in CB oxidation and have been attributed to paramagnetic sulphur compounds [16].

Table 2 Spectral parameters of X and Y signals

Sample	*g*-factor	ΔH_{pp}/G	Relative integral intensity normalized for sample mass
CB+Y-10 (after test)	2.2557	1017	6
CB+3%Cu/Y-10 (after test)	2.3505	1153	72

In EPR spectrum of Y-10 used in CB oxidation, it was found that intensities of A and B signals have become significantly lower. This allows to suppose that the admixture Fe^{3+} and Cu^{2+} ions are reduced by carbon during the reaction. On the contrary, amount of Zr^{3+} ions increases considerably (~10 times) in Y-10 catalyst after CB oxidation as compared with that in initial catalysts. This evidences the pronounced thermal reduction by carbon of Zr^{4+} ions during reaction in spite of the strong oxidizing atmosphere. This is in agreement with literature data [14], where it is reported that surface Zr^{3+} ions of ZrO_2 oxide are quite stable towards molecular oxygen and tend to be coordinately saturated by various adsorbing species (e.g. CO_2) rather than being oxidized.

Taking into account the trend of above ions to be thermally reduced by carbon, one can suppose that the change of paramagnetic form of copper in 3%Cu/Y-10 used catalyst, is related to the reduction of supported copper species by carbon during the CB oxidation and apparition of the new ones due to copper–carbon or/and copper– sulphur complexes. This might confirm the fact that the reaction is implemented through a redox mechanism with participation of supported copper metals. In accordance with reported data [3, 17], Cu^{2+} ions are the active sites of 3%Cu/Y-10 catalyst.

Conclusions

The temperature of CB combustion was decreased in the presence of all the catalysts, $10Y_2O_3$–$10CeO_2$–$80ZrO_2$ or copper loaded $10Y_2O_3$–$10CeO_2$–$80ZrO_2$. The catalytic activity strongly increased in the presence of copper. Moreover, it is correlated with the content of supported metal, that was partly related to the CuO formation. The catalytic oxidation of CB was found to occur by two successive stages mainly related to oxidation of carbon particles, and appearance of fast process during DTA was attributed to a runaway reaction. A pronounced reduction of Zr^{4+} species was also evidenced after the catalytic test. In addition the new EPR signals, appeared in the used catalysts, are attributed to the presence of paramagnetic metal–carbon or/and metal–sulphur complexes, the quantity of these complexes considerably increased with increase of the presence of copper in solids.

* * *

The European Community (European Regional Development Fund) and the region Nord-Pas de Calais are gratefully acknowledged for financial supports in purchasing the apparatus for catalytic tests.

References

1 J. P. A. Neeft, O. P. Van Pruissen, M. Makkee and J. A. Moulijn, Stud. Surf. Sci. Catal., 96 (1995) 549.
2 J. A. Moulijn, J. P. A. Neeft and M. Makkee, Appl. Catal. B, 8 (1996) 57.
3 C. Pruvost, J. F. Lamonier, D. Courcot, E. Abi Aad and A. Aboukaïs, Stud. Surf. Sci. Catal., 130 (2000) 2159.
4 G. Mul, J. P. A. Neeft, F. Kapteijn, M. Makkee and J. A. Moulijn, Appl. Catal. B, 6 (1995) 339.

5 B. A. A. L. van Setten, R. van Dijk, S. J. Jelles, M. Makkee and J. A. Moulijn, Appl. Catal. B, 21 (1999) 51.
6 B. R. Stanmore, J. F. Brilhac and P. Gilot, Carbon, 39 (2001) 2247.
7 S. P. Kulyova, E. V. Lunina, V. V. Lunin, B. G. Kostyuk, G. P. Muravyova, A. N. Kharlanov, E. A. Zhilinskaya and A. Aboukaïs, Chem. Mater., 13 (2001) 1491.
8 M. Labaki, S. Siffert, J. F. Lamonier, E. A. Zhilinskaya and A. Aboukaïs, Appl. Catal. B, 43 (2003) 261.
9 Z. Sarbak and K. Surma, J. Therm. Anal. Cal., 72 (2003) 159.
10 S. Vallová, V. Slovák and J. Leško, J. Therm. Anal. Cal., 71 (2003) 875.
11 J. P. A. Neeft, F. Hoornaert, M. Makkee and J. A. Moulijn, Thermochim. Acta, 287 (1996) 261.
12 P. Ciambelli, P. Corbo, P. Parrella, M. Scialň and S. Vaccaro, Thermochim. Acta, 162 (1990) 83.
13 J. Matta, J.-F. Lamonier, E. Abi-Aad, E. A. Zhilinskaya and A. Aboukaïs, Phys. Chem. Chem. Phys., 1 (1999) 4975.
14 C. Morterra, E. Giamello, L. Orio and M. Volante, J. Phys. Chem., 94 (1990) 3111.
15 N. Sergent, J.-F. Lamonier and A. Aboukaïs, Chem. Mater., 12 (2000) 3830.
16 C. Decarne, Ph.D. Dissertation, Dunkerque, University of Littoral, 2002.
17 D. Courcot, E. Abi-Aad, S. Capelle and A. Aboukaïs, Stud. Surf. Sci. Catal., 116 (1998) 625.